Budapest University of Technology and Economics

Faculty of Civil Engineering

Department of Engineering Geology and Geotechnics

Strength and Deformation Characteristics of Rigid Rocks under Different Conditions using Experimental Methods and Statistical Analyses

Ph. D. Thesis Booklet

Seyed Morteza Davarpanah

Supervisor:
Dr. Balázs Vásárhelyi

Budapest, April 2023

Contents

1. INTRODUCTION

Understanding the quality of the intact rock is one of the essential parts of any engineering project in rock mechanics. Accurate determination of unconfined compressive strength and Young's modulus are critical in rock engineering practice (Gercek 2007; Yagiz 2009; Dincer et al. 2004; Patel and Martin 2018; Lógó and Vásárhelyi 2019; Xiong et al. 2019; Yang et al. 2016; Zhao et al. 2017; Ranjith et al. 2004; Rahimi and Nygaard 2018)

Several papers address the impact of water on the strength of rocks by Vásárhelyi (2005), Vásárhelyi & Ván (2006), Vásárhelyi & Davarpanah (2018) and Wong et al. (2016). Li et al. (2020). However**,** there is limited research on the effect of freezing on the mechanical properties of intact rock and rock mass. Török et al. (2018) investigated the relationship between the mechanical and physical properties of two highly porous rocks, such as oolitic Miocene limestone and Miocene rhyolite tuff. It was observed that the strength of the ice, dry and water-saturated porous rocks are relatively low, but when the rocks are frozen, very high uniaxial strength values are measured (Davarpanah et al. 2021)

Significant strength increase was observed in several rock types with subzero temperatures. Similarly, in the paper by Davarpanah et al. (2019), the relationship between different mechanical properties of highly porous limestone in dry, water-saturated, and frozen conditions (-20 °C) was investigated. It was found that the mechanical behaviour of the frozen rock is significantly different from saturated and air-dry specimens, having higher strength and modulus of elasticity. Yang et al. (2018) investigated the mechanical properties of frozen rock mass with two diagonal intersected fractures and concluded that the dips of two fractures significantly influenced the results.

Mellor (1971, 1973) measured the uniaxial compressive and tensile strengths of water-saturated and air dry granite, limestone, and sandstone rock core from temperatures of 25 to -195ºC. Mellor observed that the compressive strengths increase with decreasing temperature. As the temperature drops, mineral grains shrink, and ice formation in pore spaces contributes directly to the strength of the material. Freezing was noted to increase rock strength by 4 in porous rock and 1.8 in crystalline rock. Also, Young's modulus increases with a decrease in temperature; however, a further reduction in temperature from -10 to -20 C does not affect Young's modulus, according to Yamabe & Neaupane (2001).

Glamheden and Lindblom (2002) investigated frozen rock mass properties and completed numerical modelling for an unlined hard rock cavern measuring 7m in diameter and 15 m high in Gothenburg, Sweden. It was observed that tensile strength increases with decreasing temperature, and Young's modulus and Poisson's ratio marginally increase at decreasing temperature. In practical case studies, the application of freezing to improve rock mass quality was reported by Wardrop (2005) for several underground mines in Russia and Canada. According to the reports, significant improvement was observed in RMR and Q due to freezing.

Roworth (2005) conducted a series of USC tests on three different rocks (hematized sandstone, bleached sandstone, and metapelaite basement). Based on his observations, there was a significant gain in strength due to freezing. The weakest rock samples are expected to have the most significant increase in strength due to freezing. He also established the link between the stress-strain behaviour of tested samples and freezing temperature. Frozen earth exhibits time

and temperature-dependent rheological behaviour. In other words, the strength is based on the rock's temperature and the loading duration.

Kodama et al. (2019) investigated the long-term behaviour of Shikotsu welded tuff at subzero temperatures. The results illustrated that the uniaxial compressive strengths of frozen wet specimens were greater than those of the frozen dry samples; however, frozen wet specimens experienced shorter creep lives than frozen dry specimens. Moreover, the strains of the frozen wet specimens were much more significant than those of the frozen dry specimens. It is associated with the time dependence of the mechanical behaviour of pore ice. In addition, the UCS of a frozen wet specimen can be more significant because the fracture initiation stresses of the pores in the frozen wet specimen are more significant on average than those in a frozen dry sample. In another similar work published by Liu et al. (2020), crack initiation stress and crack damage stress increased due to freezing in sandstone and mudstone. The reason is that pore ice reduces stress concentration around a crack and enhances the cementation of mineral particles. Therefore, peak stresses of sandstone and mudstone increase linearly with the decrease in freezing temperature.

Davarpanah et al. 2022, published a review paper on the mechanical behaviour of frozen rocks and compared the different mathematical models for frozen rock behaviour. According to their results, gain and increase in strength and deformation of rocks are material dependent.

This dissertation is intended to discuss the strength and deformation behaviour of different rocks and the influence of saturation and freezing on these mechanical properties. The outline of this research consists of 8 new scientific results, which will be discussed in the following parts.

2. OBJECTIVES

The goal of the first part of this research (new scientific result 1, new scientific result 2, new scientific result 3, and new scientific result 4) is to present changes in the physical and mechanical properties of porous rocks due to saturation and freezing. For this purpose, different kinds of rocks, such as highly porous Miocene limestone (65 samples) and porous rhyolite tuff (17 samples), and marl (120 samples), were prepared and analyzed. The samples were examined in various conditions, including air, saturated water, and freezing temperatures (-20 °C). The laboratory tests included determining density, ultrasound speed propagation, porosity, capillary water absorption, and strength parameters. Regression analyses were used to examine the measured physical and mechanical parameters. The main objective of the second part (new scientific result 5, new scientific result 6, and new scientific result 7, new scientific result 8) is to investigate the relationships between strength and deformation behavior (uniaxial compressive strength (σ_c), tensile strength (σ_t), Poisson's ratio (υ) and Young modulus(E) for different igneous, sedimentary and metamorphic rocks such as siltstones, sandstones, quartzites and limestone. Also, granitic rock samples (50 samples) were collected from Bátaapáti radioactive waste repository and the values of crack initiation stress (σ_{ci}) and crack damage stress (σ_{cd}) were calculated based on existing approaches (Brace et al. 1966; Martin et al. 1994; Diederichs 2007). Moreover, the link between various static and dynamic deformation moduli was investigated, and the results show a well-fit nonlinear relationship between deformation

moduli. Finally, a detailed analysis was undertaken on the quasi-isotropic intact rock to compute the value of m_i and compare the results to propose new material model constants that best fit the experimental data.

3. MATERIALS AND METHODS

3.1. The effect of water saturation on the mechanical properties of limestone

This part analyzes many laboratory tests of high porosity Hungarian miocene limestones to examine the effect of water content on uniaxial compressive strength, tensile strength, Young modulus, rigidity, etc., Hoek-brown material constant and Mohr-Coulomb parameters. The ratio of the elastic modulus and the uniaxial compressive strength of the intact rock is also calculated. According to the laboratory results, this ratio (namely the modulus ratio) is independent of the water content.

3.2. Changes in physical and mechanical properties of highly porous limestone

Thirty-five cylindrical, highly porous limestone specimens were drilled from stone blocks for the tests. The samples were between 48.2 and 48.8 mm in diameter and 83.3 and 97.6 mm in height. Twenty-one samples were used for the uniaxial compressive test, and the others were selected for Brazilian test. Samples were categorized into three groups, dry, saturated and frozen. The tests were carried out in different petrophysical states (i.e. dry, water-saturated and frozen states after water saturation). Ultrasonic pulse velocity was measured on all specimens, and water absorption tests were recorded on selected samples. The frozen samples were tested on water-saturated rock samples cooled to -20 °C. The tests were made according to ISRM's (1985, 2007) suggested methods.

3.3. Physical and mechanical properties of dry, saturated and frozen porous limestone and tuff samples

Two highly porous rocks were studied: Miocene limestone and Miocene rhyolite tuff. Two lithotypes of Miocene limestone from the Sóskút quarry were chosen for the tests: a medium-grained and a coarse-grained bioclastic one that contains shell fragments. Cylindrical test specimens of 5 cm diameter were used for the laboratory tests. Density and ultrasonic pulse wave velocity were measured in different petrophysical states (i.e. dry, water-saturated and frozen states after water saturation). The frozen samples were tested on water-saturated rock samples cooled to −20 °C. Unconfined compressive tests measured the strength and Young's modulus. The laboratory investigations were carried out according to ISRM's (1985, 2007) suggested methods (Ulusay and Hudson 2006).

3.4. Physical and mechanical characteristics of marl samples under freezing

The laboratory tests included firstly non-destructive tests, such as the measurements of density and ultrasonic pulse wave velocities in different petrophysical states and destructive tests, such as Uniaxial Compressive Strength (UCS), the tensile strength (using Brazilian test) and point load test (PLT). To determine the mechanical properties of investigated rock samples, 39 cylindrical marl samples were prepared (but three samples failed in the water saturation stage before the test), so 36 samples were available for the uniaxial compressive test, from which 12 samples in dry condition, 11 samples in saturated condition and 13 samples in frozen

condition were tested. The samples were between 49 and 49.72 mm in diameter and 75 and 107.18 mm in height. Similarly, 42 samples were cut for the Brazilian test, but 36 test was carried out. After performing the Brazilian test, half-cut broken tensile test samples were used for the PLT test. Forty-eight-point load tests were carried out. The frozen samples were tested on water-saturated rock samples cooled to -20 °C. The tests were made according to ISRM's (1985, 2007) suggested methods.

3.5. Investigation of the strength and deformation characteristic of Mórágy Granitic rock

Laboratory samples originated from research boreholes deepened in the carboniferous Mo'ra'gy Granite Formation during the research and construction phases of a deep geological repository of low and intermediate-level radioactive waste. This granite formation is a carboniferous intruded and displaced Variscan granite pluton in South-West Hungary. Fifty uniaxial compressive tests were performed in the rock mechanics laboratory at RockStudy Ltd. The D = 50 mm cylindrical rock samples with the ratio L/D = 2/1 (here, L and D are the length and diameter of a model, respectively) were prepared. The samples were tested using a computer-controlled servo-hydraulic machine in continuous load control mode. The loading magnitude was settled in kilonewton with 0.01 accuracy, and the loading rate was 0.6 kN/s. Axial and tangential deformation was measured by strain gauges, which measure the deformation between 1/4 and 3/4 of the sample's height. Moreover, crack initiation stress (σ_{ci}) and crack damage stress (σ_{cd}) were calculated based on the Onset Dilatancy Method, Crack Volumetric Strain Method, and Change of Poisson's Ratio Method (Brace et al. 1966; Martin et al. 1994; Diederichs 2007).

3.6. Nonlinear regression analyses between static and dynamic deformation moduli of different kinds of rocks

There are several relationships between the static and dynamic Young's moduli (Belikov et al. 1970; King 1983; Eissa and Kazi 1988; McCann and Entwisle 1992; Eissa and Kazi 1988; Christaras et al. 1994; Nur and Wang 1999; Brotons et al. 2014; Brotons et al. 2016). These equations can be divided into linear and nonlinear groups. For this study, 40 samples of different rocks (igneous, sedimentary and metamorphic) from the literature were analyzed (Lama and Vutukuri 1978). Data were classified according to rock types, and the relationship between dynamic and static constants was investigated statistically.

3.7.Determination of Young's Modulus and Poisson's Ratio for Intact Stratified Rocks

The rock materials discussed in this part are from the surface and underground mining projects in two distinctly different geological, environmental, and climatic settings. In Project 1, weathered to fresh, calcareous, and argillaceous siltstones, sandstones, and quartzites from Proterozoic stratigraphy in the Yeneena Supergroup are found from the surface down to approximately 1,200 metres depth in the Great Sandy Desert of Western Australia (Nicoll et al. 2017; Bar and Weekes 2017). Surface weathering decreases quite rapidly with depth. In Project 2, fresh siltstone (Cretaceous) and limestone (Eocene to Miocene) strata are repeated due to thrust faulting from the surface down to 1,500-meters depth in the Western Province of Papua New Guinea (PNG), a high rainfall, tropical region.

3.8.Characterization of Hoek–Brown constant m_i for quasi_isotropic intact rock

Although several practical, empirical, and probabilistic approaches have been presented in the literature to address uniaxial compressive strength (UCS) (Davarpanah et al. 2020, Hoek and Brown 1997, Hoek et al. 2013, Vásárhelyi and Kovács 2016, and Wen et al. 2020], the accurate determination of m_i is still challenging task. Many factors influence it, such as mineral composition, grain size, and rock cementation. Generally, m_i presents a curve-fitting parameter for the Hoek-Brown failure envelope (Hoek and Marinos 2000). So far, different approaches such as the rigidity index method (R-index), uniaxial compressive strength (UCS) based method, and tensile strength (T.S.) based practice, and the combination of these two methods (Combination based method) have been proposed for calculating the value of m_i. This study aims to thoroughly review the previously existing procedures to calculate the value of m_i and compare the obtained results to propose the new material constants that best fit the experimental data.

4. NEW SCIENTIFIC RESULTS(NSR)

4.1. NEW SCIENTIFIC RESULT (1)

Based on statistical analyses, due to water saturation, both the uniaxial compressive strength and tensile strength decrease similarly; However, the ratio of these two values is constant. Thus, the internal friction angle does not change but only the cohesion. Likewise, the Hoek-Brown constant (m_i) remains constant, independent of the moisture content (Vásárhelyi and Davarpanah 2018).

According to the laboratory test results, different mechanical parameters decrease due to the increased moisture content of the rock. Hawkins and McConnell (1992) investigated the influence of the moisture content on the strength of the rock, and they suggested the following form:

$$\sigma_c(w) = a e^{-bw} + c \,, \qquad (1)$$

Where $\sigma_c(w)$ is the uniaxial compressive strength (MPa), w is the water content (%), and a, b and c are constants.

According to the Coulomb failure criteria, the internal friction angle (ϕ) can be calculated from the ratio of the uniaxial compressive strength (σ_c) and the tensile strength (σ_t):

$$R = \frac{\sigma_c}{|\sigma_t|} = \frac{1+\sin\phi}{1-\sin\phi} \qquad (2)$$

As shown before, this ratio is independent of the water ratio. Thus, the internal friction angle is a material constant, not influenced by the moisture content.

Cai (2010) showed that m_i constant in the Hoek-Brown failure criterion is equal to the ratio of UCS (σ_c) to tensile strength (σ_t) (see Eq. 2). According to the calculation of Cai (2010), when $R \geq 8$, the error for approximating m_i by R (is less than 1.6 %; thus, the Hoek-Brown parameter (m_i) can be calculated using the following form (Eq.3)

$$m_i \approx R = \frac{\sigma_c}{|\sigma_t|} \quad (3)$$

According to Hoek (2007), m_i values range from 4 to 33 for some commonly encountered rocks in engineering practice, and m_i depends on many factors such as mineral contents, foliation and grain size (texture) – but as it was shown previously, m_i value is independent on the water content.

4.2. NEW SCIENTIFIC RESULT (2)

I experimentally proved that freezing causes an increase in mechanical properties such as uniaxial compressive strength, tensile strength and Young's modulus of highly porous limestone. In contrast, these parameters experience a decrease due to saturation (Davarpanah et al. 2020a)

Typical stress-strain curves of highly porous limestone are very different for dry, water-saturated and frozen specimens (Fig. 1). The maximum uniaxial compressive strength of samples in the frozen condition is about 13 MPa, and 3.5, and 2.7 MPa in dry and saturated, respectively. Namely, the strength in the frozen condition is about 80 % more than in dry and 65 % more than in saturated conditions.

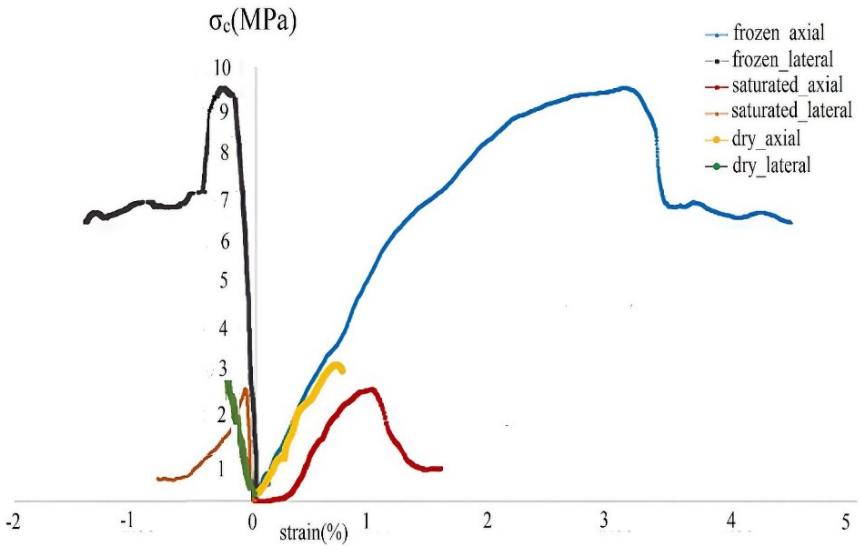

Fig. 1. Typical stress-strain curves of highly porous limestone (Davarpanah et al. 2020a)

4.3. NEW SCIENTIFIC RESULT (3)

I experimentally proved that mechanical properties such as uniaxial compressive strength, tensile strength, and Young's modulus of porous limestone and tuff increase due to freezing but decrease due to saturation (Davarpanah et al. 2020a, Davarpanah et al. 2022).

The tests of frozen porous limestone and rhyolite tuff samples disproof the idea that in frozen rocks, the ice, with its crystallization pressure, cause micro-cracking and leads to a lower compressive strength. On the contrary, much higher strength was measured on frozen porous rocks (limestone, bioclastic limestone and rhyolite tuff). The ice has a strength close to the

samples' water-saturated strength values. Thus, the strength of the ice, dry, and water-saturated porous rocks is relatively small, but when the rocks are frozen, these strength values are 'added' to each other, and very high uniaxial strength values are measured. These experiments have proved that the uniaxial compressive strength of porous rocks can be significantly increased by freezing (Fig. 2); accordingly, freezing can stabilize porous rock masses around tunnels or deep foundations.

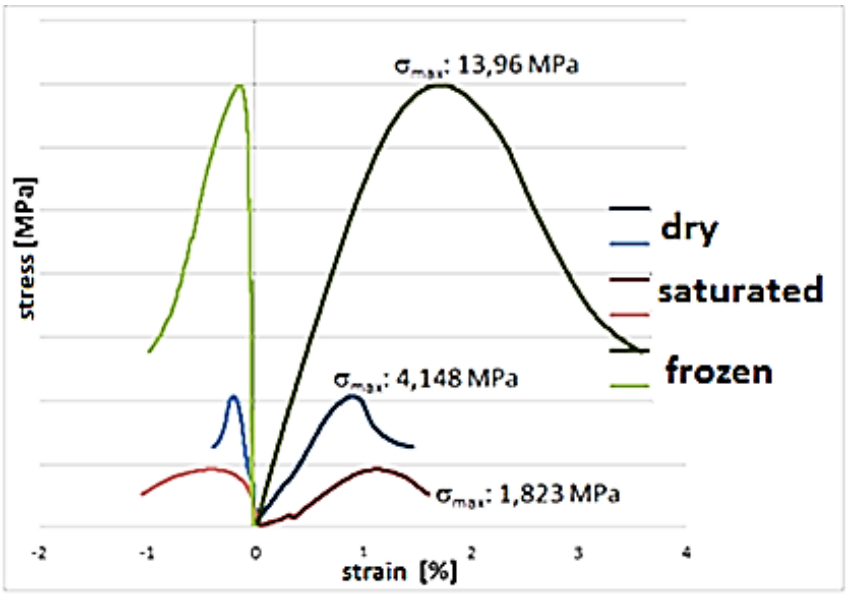

Fig.2.Typical stress-strain curves of the rhyolitic tuff (Davarpanah et al. 2022)

4.4. NEW SCIENTIFIC RESULT (4)

I experimentally proved that the mechanical properties such as uniaxial compressive strength, tensile strength and Young's modulus of frozen saturated marls significantly increase due to freezing (Davarpanah et al. 2021a).

A typical stress-strain curve of studied marl specimens is very different under dry, water-saturated, and frozen conditions (Fig. 3). As it is evident, with the reduction of temperature, the compaction stage can be shortened. The slope of the elastic stage increases, and then yield phenomenon becomes more and more unobvious, which means increases in elastic modulus and brittleness. Frozen samples' average uniaxial compressive strength is 21.93 MPa, 86% more than saturated ones (11.76 MPa). Under freezing conditions, the cementation of the ice and particles improves the integrity of the rock mass, making the rock viscoplastic and brittle. Moreover, rock mass strength is thought to increase in frozen rock because of the fracture initiation stress, which follows the elastic deformation region due to a reduction in the stress concentration in the pores or interstitial spaces within the rock.

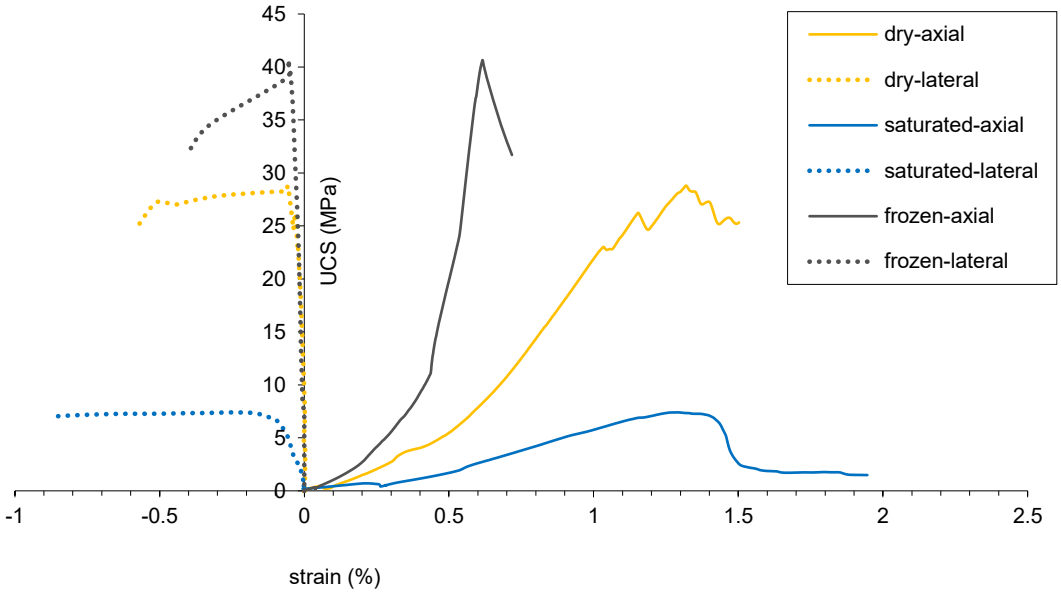

Fig. 3. A typical stress-strain curve under dry, saturated, and frozen conditions (Davarpanah et al. 2021a)

4.5. NEW SCIENTIFIC RESULT (5)

I experimentally proved that the proposed model by Palchik (2019) for very strong limestones and dolomites is in good agreement with the elastic region of stress-strain relationships observed in this study for very strong granitic rock samples. However, there is a significant difference in the non-linear part of stress-strain relationships between the observed and estimated values (Davarpanah et al. 2019, Davarpanah et al. 2020b).

Palchik (2019) proposed a simple stress-strain model for very strong ($\sigma_c > 100\ MPa$) carbonate rocks based on Haldane's distribution function (Haldane 1919).

$$\sigma_a = \sigma_c\left(\frac{1-e^{-s\varepsilon_a}}{1-e^{-\theta}}\right) \quad (4)$$

Where σ_a is current axial stress (MPa), ε_a is a current axial strain (%) at the axial stressσ_a, σ_c is a uniaxial compressive strength (MPa), parameter (s) is a constant involved in a canonical form of Haldane's function. For very strong limestones and dolomites ($\sigma_c > 100\ MPa$) the value of s is between 0.5 and 1, and exponent θ is defined as follows

$$\theta = -ln\left[1 - \frac{\sigma_c}{\sigma_a}(1 - e^{-0.5\varepsilon_a})\right] \quad (5)$$

And can be presented in the following form by using Taylor's series expansion:

$$\theta = \emptyset + \frac{\emptyset^2}{2} + \frac{\emptyset^3}{3} \quad (6)$$

$$\emptyset = \left(\frac{\sigma_c}{\sigma_{a1}}\right)(1 - e^{-0.5\varepsilon_{a1}}) \quad (7)$$

when s = 1.1:

$$\sigma_a = \sigma_c\left(\frac{1-e^{-1.1\varepsilon_a}}{1-e^{-\psi}}\right) \quad (8)$$

$$\psi = -ln\left[1 - \frac{\sigma_c}{\sigma_a}(1 - e^{-1.1\varepsilon_a})\right] \quad (9)$$

$$\psi = \upsilon + \frac{\upsilon^2}{2} + \frac{\upsilon^3}{3} \quad (10)$$

$$\upsilon = (\frac{\sigma_c}{\sigma_{a1}})(1 - e^{-1.1\varepsilon_{a1}}) \quad (11)$$

The estimated and observed stress-strain relationships for four granitic rock samples are presented in Fig. 4.

Sample(a1):$\sigma_c = 181.05\ MPa$, $\sigma_{a1} = 27.8\ MPa$ at $\varepsilon_{a1} = 0.037\%$

Sample(b4): $\sigma_c = 184.48\ MPa$, $\sigma_{a1} = 22.22\ MPa$ at $\varepsilon_{a1} = 0.042\%$

Sample(c6): $\sigma_c = 148.39\ MPa$, $\sigma_{a1} = 34.44\ MPa$ at $\varepsilon_{a1} = 0.045\%$

Sample(d8): $\sigma_c = 204.23\ MPa$, $\sigma_{a1} = 28.93\ MPa$ at $\varepsilon_{a1} = 0.032\%$

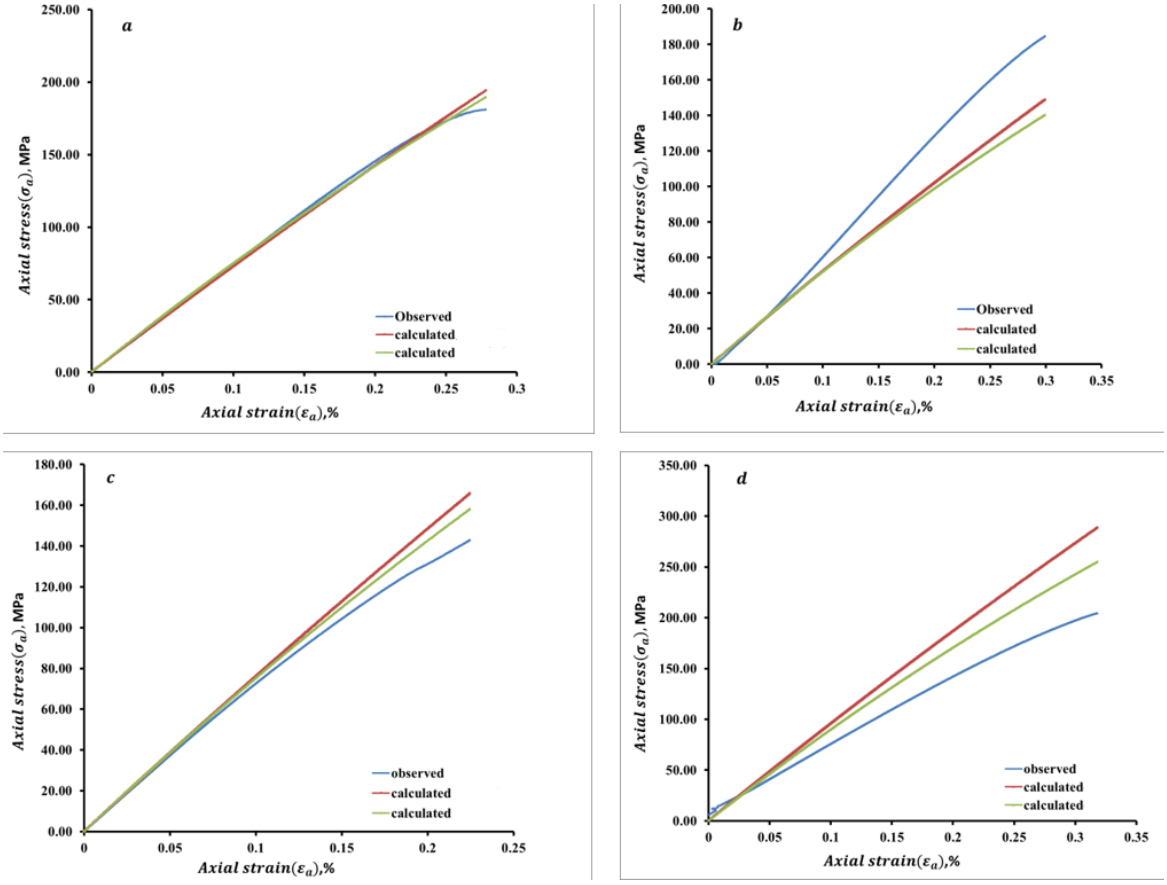

Fig. 4. Examples of comparison of stress-strain models [Eqs. (4), (8)] and stress-strain relationships observed in this study for very strong (σ_c > 100 MPa) granitic rock samples (a, b, c, d) (Davarpanah et al. 2020b)

4.6. NEW SCIENTIFIC RESULT (6)

According to regression analyses, new linear and nonlinear correlations were established between static and dynamic Young's modulus of different rocks (Davarpanah et al., 2020c).

Fig.5 and 6 show the logarithmic, power and linear regression analysis between static and dynamic modulus of elasticity for different rock types. Based on our analyses, we received the correlations with high determination coefficients. for igneous rocks, the value of R^2 = 0.96; for sedimentary rocks, the value of R^2 = 0.91; for metamorphic rocks, the value of R^2 = 0.63.

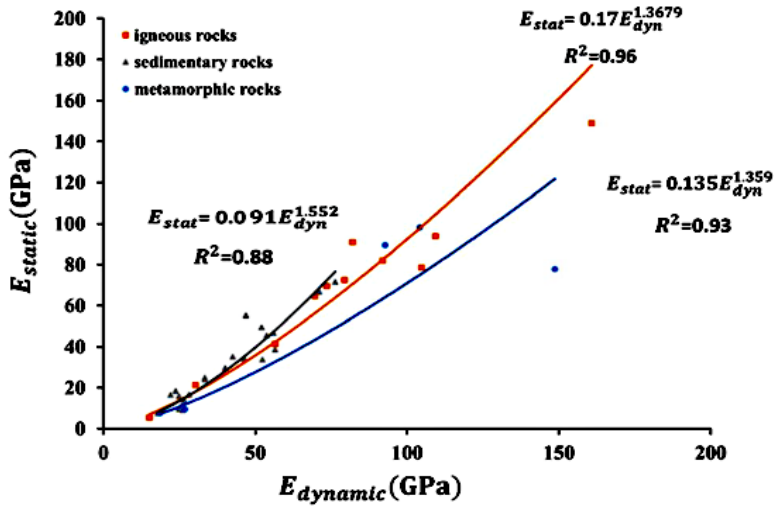

Fig. 6.. Relationship between static and dynamic modulus of rigidity based on rock types (Davarpanah et al. 2020c)

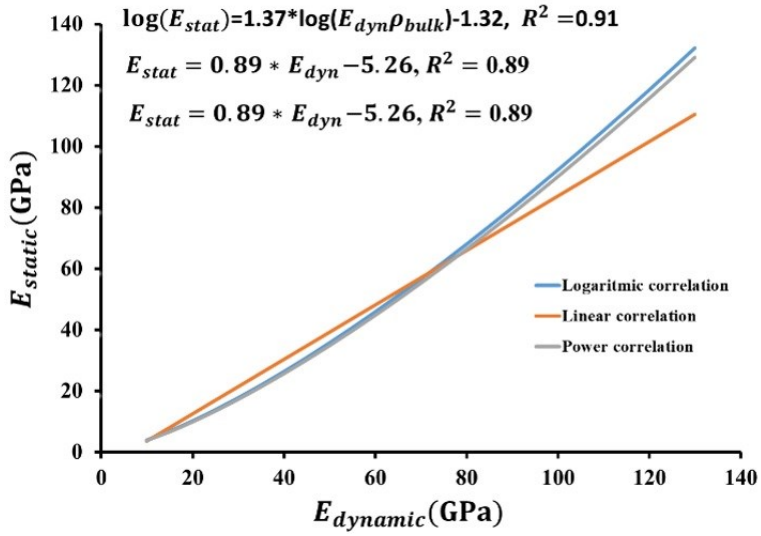

Fig. 5. Linear and nonlinear achieved correlations for all rock types (Davarpanah et al. 2020c)

4.7. NEW SCIENTIFIC RESULT (7)

According to our statistical analyses, new linear correlations have been published between deformation constants of different rocks (Davarpanah et al., 2020d).

The relationships between secant and tangent Young's modulus (E), shear modulus (G) and bulk modulus (K), and uniaxial compressive strength (σ_c) are displayed. As shown Fig 6 and

Fig. 7, there is a correlation with the value of ($R^2 = 0.52$) between secant and tangent Young's modulus and uniaxial compressive strength. Fig. 8 and Fig. 9 exhibits the correlation between secant and tangent Young's modulus with the value of ($R^2 = 0.51$). Nevertheless, in Fig. 10 and Fig.11, when we calculate the bulk modulus, there is a significant decrease in correlation, which declined to (R2 = 0.22). So far, different relationships between tangent Young's modulus and uniaxial compressive strength have been published in the literature (Table).

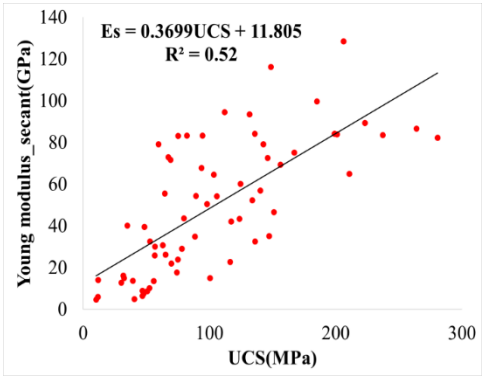

Fig. 6 Relationship between Es-UCS

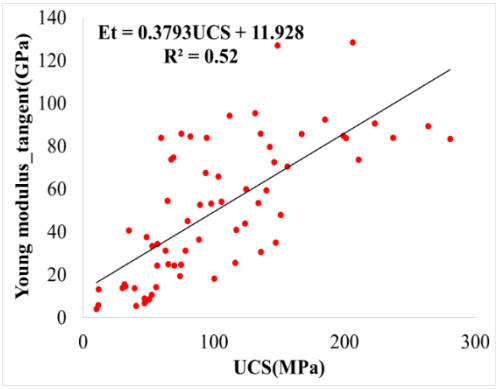

Fig. 7 Relationship between Et-UCS

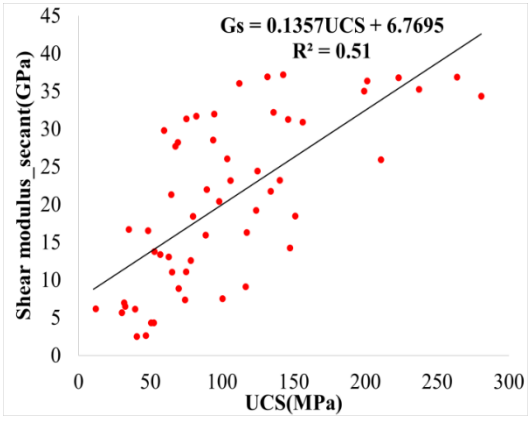

Fig. 8 Relationship between Gs-UCS

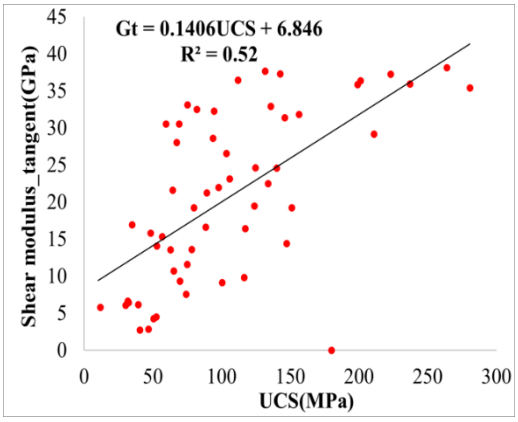

Fig. 9 Relationship between Gt-UCS

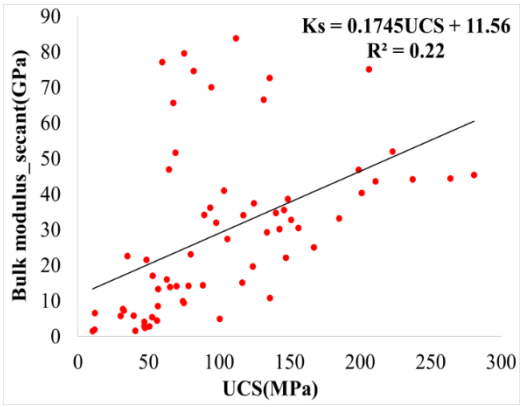

Fig. 10 Relationship between Ks-UCS (Davarpanah et al. 2020d)

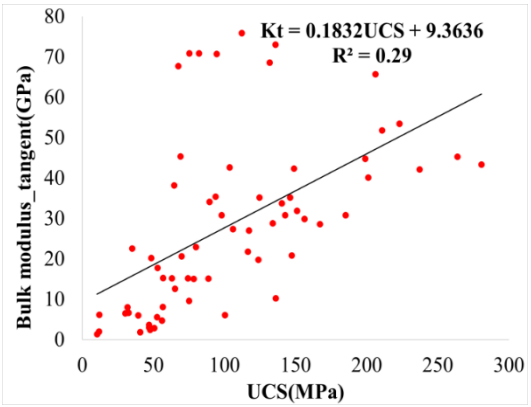

Fig. 11 Relationship between Kt-UCS (Davarpanah et al. 2020d)

Table 1 Correlations between unconfined compressive strength (MPa) with tangent Young's modulus (GPa*) (Davarpanah et al. 2020d)*

Rock type	Equation	R^2	Reference
Sandstone	$E_t = 0.28UCS + 5.83$	0.80	Wuerker (1959)
shale	$E_t = 0.28UCS^{0.87}$	0.89	Wuerker (1959)
Sandstone	$E_t = 0.19UCS + 4.86$	0.93	Dhir and Sangha (1978)
Limestone	$E_t = 0.97UCS^{0.69}$	0.87	Dhir and Sangha (1978)
Dolomite	$E_t = 0.15UCS + 21.6$	0.44	Lama and Vutukuri (1978)
Shale	$E_t = 1.93UCS^{0.63}$	0.55	Lama and Vutukuri (1978)
Sandstone	$E_t = 0.31UCS$		Wilson (1980)
Marble	$E_t = 1.06UCS^{0.72}$	0.86	Wilson (1980)
Sandstone	$E_t = 0.13UCS + 3.42$	0.71	Dennis et al. (1982)
Bituminous schist	$E_t = 0.15UCS^{0.76}$	0.78	Dennis et al. (1982)
Sandstone	$E_t = 0.28UCS + 12.5$	0.35	Bell (1983)
Siltstone Shale	$E_t = 1.24UCS^{0.78}$	0.90	Bell (1983)
Limestone	$E_t = 0.25UCS + 15.5$	0.85	Sachpazis (1990)
Dolomite	$E_t = 0.5UCS^{0.95}$	0.95	Sachpazis (1990)

Sandstone	$E_t = 0.05UCS + 20.6$	0.29	Rohde and Feng (1990)
Sandstone	$E_t = 2.25UCS^{0.52}$	0.5	Rohde and Feng (1990)
Gypsum	$E_t = 0.27UCS + 19.08$	0.81	Arslan et al (2008)
Gypsum	$E_t = 10.52UCS^{0.28}$	0.78	Arslan et al. (2008)
Sandstone	$E_t = 0.17UCS$	0.73	Vásárhelyi(2003)
Sandstone	$E_s = 0.14UCS$	0.75	Vásárhelyi(2003)

4.8. NEW SCIENTIFIC RESULT (8)

According to statistical analyses, new material models are published to determine the Hoek-Brown material constant (m_i), which provides the best fit with experimental data (Davarpanah et al., 2021b, Davarpanah et al., 2023).

Comparing the published values of mi by (Ván and Vásárhelyi 2014) with the guidelines (Cai 2010, Hoek 2007, and Hoek and Brown 1980) given for igneous rocks, the value of mi for basalt is between 20 and 30. In contrast, the minimum published value of mi for Basalt is 4.31, which does not fall within the expected range. The minimum published value of mi for basalt is even less than for volcanic tuffs. The latter one is between 8 and 13. The published mi values for granite are between 11.68 and 34.03, but the expected range based on the guidelines is between 29 and 35. The same discrepancy was observed for gabbro. Based on the guideline values, the predicted range is between 24 and 30, whereas the published results are between 15.31 and 20.74. Our developed model with new material constants for Hoek-brown m_i determination provides the best fit with experimental data. Based on the empirical model by Wen et al. 2020, most of the estimated values of mi are within the upper/lower limit of 90 %, which accounts for 96.6 % of all the data, and all the calculated values are within the upper/lower limit of 80 %. This result indicates that the developed relation estimates of mi agree well with the experimental observations, demonstrating that the developed relation can estimate mi accurately. The comparison graph between our results and the recently published paper by Wen et al. 2020 is presented in Fig. 8.

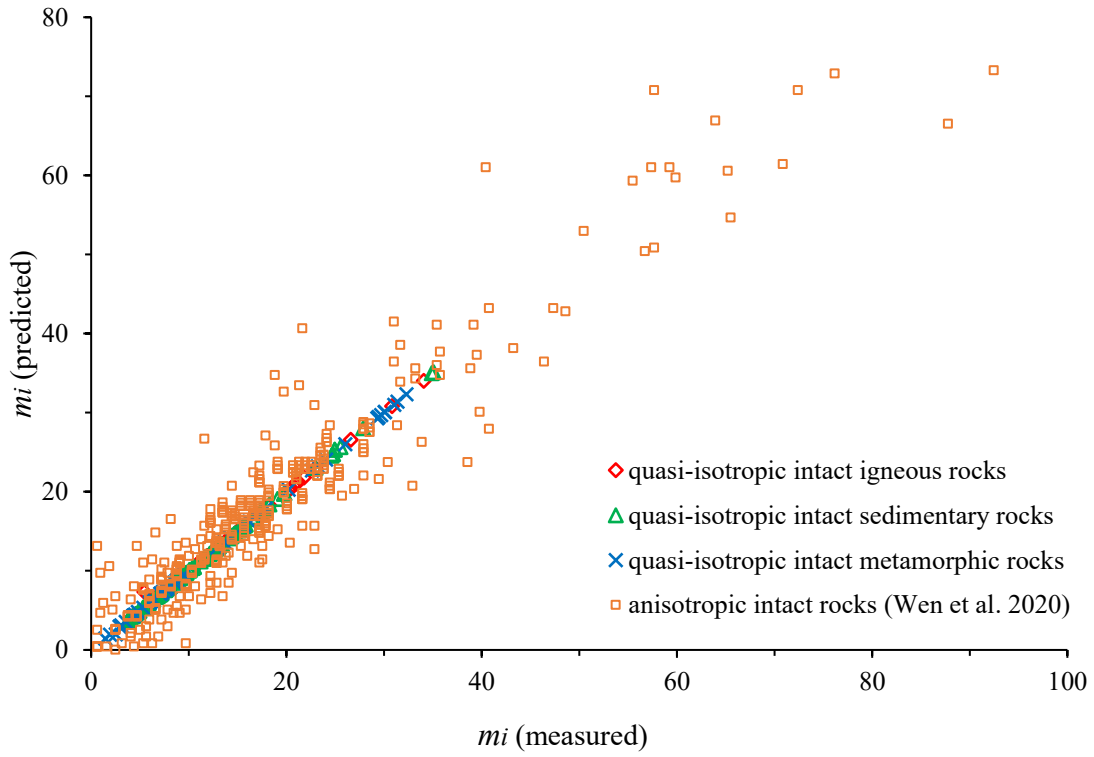

Fig. 8. Comparison between mi values estimated (Wen et al 2020) via the proposed relation and measured values for different rock types (red rhombus symbol is related to quasi-isotropic intact igneous rocks; green triangle symbol is related to quasi-isotropic intact sedimentary rocks; blue cross symbol is related to quasi-isotropic intact metamorphic rocks; and small orange square symbol is related to anisotropic intact rocks (Davarpanah et al. 2021b)

5. LIST OF PUBLICATIONS (2017-2022)

Journal papers

1. **Davarpanah, M.,** Narimani, S., Sharghi, M., Vásárhelyi, B. Török, Á. (2023): Brittle-Ductile Transition Stress of Different Rock Types and Its Relationship with Uniaxial Compressive Strength and Hoek-Brown Material Constant. *Sci Rep* ***13****, 1186* https://doi.org/10.1038/s41598-023-28513-3, IF: 4.99, **Q1**
2. **Davarpanah, M.,** Török, Á Vásárhelyi, B. (2022): Review on the mechanical properties of frozen rocks. Mining-Geology-Petroleum Engineering Bulletin. https://doi.org/10.17794/rgn.2022.3.7. IF: 1.59, **Q2**
3. **Davarpanah, M.,** Sharghi, M., Tarifard, A. Vásárhelyi, B., Török Á. (2021a): Studies on the Mechanical Properties of Dry, Saturated, and Frozen Marls Using Destructive and Non-destructive Laboratory Approaches. Iran J Sci Technol Trans Civ Eng. https://doi.org/10.1007/s40996-021, IF: 1.47, **Q2**
4. **Davarpanah, M.,** Sharghi, M., Vásárhelyi, B. Török, Á. (2021b): Characterization of Hoek–Brown constant m_i of quasi-isotropic intact rock using rigidity index approach. *Acta Geotech.* https://doi.org/10.1007/s11440-021-01229-2, IF: 5.94, **Q1**
5. **Davarpanah M.**, Török Á., Vásárhelyi B. (2020a): *Investigation of the mechanical properties of dry, saturated and frozen highly porous limestone*, Int. Cong. on Rock Mech. Rock Engng, September 13-18, (ISRM) Foz do Iguassu- Brazil. 2325-2332.
6. **Davarpanah, M.,** Somodi G., Kovács L., Vásárhelyi B. (2020b): Experimental determination of the mechanical properties and deformation constants of Mórágy granitic rock formation (Hungary). Geotechn. and Geol. Engng, **38**(3): 3215-3229, doi: 10.1007/s10706-020-01218-4, IF:1.54, **Q2**

7. **Davarpanah M.,** Ván P., Vásárhelyi B. (2020c): Investigation of the relationship between dynamic and static deformation constants of rocks, *Geomechanics and Geophysics for GeoEnergy and Geo-Resources*, **6**(1): 29. doi: 10.1007/s40948-020-00155-z, IF: 4.35, **Q1**
8. **Davarpnah M.,** Bar N., Török Á., Tarifard A., Vásárhelyi B (2020d): Determination of Young's modulus and Poisson's ratio for intact stratified rocks and their relationships with uniaxial compressive strength, Austrailian Gemechanics Journal,55, 4, 101-118., **Q3**
9. **Davarpanah M.,** Somodi G., Kovács L., Vásárhelyi B. (2019): Complex analysis of uniaxial compressive tests of the Mórágy granitic rock formation (Hungary). *Studia Geotechn. et Mech.*, **41**(1): 21–32. doi: 10.2478/sgem-2019-0010, IF: 1.03, **Q3**
10. Vásárhelyi B., **Davarpanah M.** (2018): Influence of water content on the mechanical parameters of the intact rock and rock mass. *Periodica Polytechnica Civil Engng*, **62**(4): 1060-1066. doi: 10.3311/PPci.12173, IF: 1.07, **Q2**

(Publications not Related to thesis)

11. Narimani, S, **Davarpanah, M.,** Kovács, L.,Vásárhelyi, B (2023.) Variation of Elastic Stiffness Parameters of Granitic Rock during Loading in Uniaxial CompressiveTest.*Appl.Mech. 4(2):445-459.* https://doi.org/10.3390/applmech4020025
12. Hallaji Dibavar B., Ahmadi M., **Davarpanah M.** (2020): 3D numerical investigation of ground settlements induced by construction of Istanbul Twin Metro Tunnels with special focus on tunnel spacing. *Periodica Polytechnica Civil Engng*, **63(**4): 1225-1234. doi: 10.3311/PPci.14591, IF: 1.07, **Q2**
13. Mohtadinia M., Ahmadi M., Manafi M. Hallaji Dibavar B, **Davarpanah, M.** (2020): Statistical and Numerical Study of Chipping and Cracking in Segmental Lining. *Periodica Polytechnica Civil Engng*, doi: 10.3311/PPci.14591, IF: 1.07, **Q2**
14. Narimani S., Chakeri H., **Davarpanah M**. (2018): Simple and non-linear regression techniques used in sandy-clayey soils to predict the pressuremeter modulus and limit pressure: a case study of Tabriz subway. *Periodica Polytechnica Civil Engng*, **62**(3): 825-839. doi: 10.3311/PPci.12063, IF: 1.07, **Q2**
15. **Davarpanah, M.,** Sharifzadeh, M., Sattarvand, J., Narimani, S. (2016) Evaluation of Building Displacement Induced By EPB Tunneling Through GPS-GNSS Monitoring System and Back Analysis Technique (Tabriz Subway Twin Tunnels), Civil Engineering Journal, https://doi.org/10.28991/cej-2016-00000032, **Q1**
16. Narimani, **S., Davarpanah, M.,** Sattarvand, J. (2016) Prediction of Hydro-mechanical Stability of Dam: Using Calibrated Model from Back Analysis and Monitoring Data, Civil Engineering Journal, https://doi.org/10.28991/cej-2016-00000044 , **Q1**
17. Ahmadi, M., Mortazavi, A., **Davarpanah, M**. Zarei, H (2016) A Numerical Investigation of Segmental Lining Joints Interactions in Tunnels-Qomrud Water Conveyance Tunnel, Civil Engineering Journal, https://doi.org/10.28991/cej-2016-00000038, **Q1**

***Conference proceedings*:**

18. **Davarpanah M.**, Narimani S., Besharatinezhad A., Khodabandeh M., Török Á., Vásárhelyi B. (2022): *Applicability of the recently proposed semi-empirical failure criterion for different rock types by using triaxial test data*, Fifth symposium of the Macedonian Association for Geotechnics, 2022 Macedonian Association for Geotechnics, ISBN 978-9989-2053-4-7.
19. Besharatinezhad A., Khodabandeh M. Narimani S., Török Á., **Davarpanah M.**, Vásárhelyi B. (2022): *Analytical and numerical investigation of the critical height of vertical rock slope*, Fifth symposium of the Macedonian Association for Geotechnics, 2022 Macedonian Association for Geotechnics, ISBN 978-9989-2053-4-7.
20. **Davarpanah M.**, Török Á., Vásárhelyi B. (2020a): *Investigation of the mechanical properties of dry, saturated and frozen highly porous limestone*, Int. Cong. on Rock Mech. Rock Engng, September 13-18, (ISRM) Foz do Iguassu- Brazil. 2325-2332.

21. **Davarpanah M.**, Vásárhelyi B., Ván P. (2019): *Investigation of relationship between dynamic and static deformation constants of rocks*, Int. Cong. on Geomathematics in Earth- & Environmental Sciences. Pecs, Hungary.
22. Ahmadi M.H., Molladavoodi H., Vásárhelyi B., **Davarpanah M**., Dibavar B.H. (2019): *A numerical Investigation of brittle rock fracture mechanism under high rate loading based on a micromechanical damage model*, ISRM Specialised Conf., Omiš – Split, Croatia,115-120.
23. Török Á., Ficsor A., **Davarpanah M.**, Vásárhelyi B. (2018): *Comparison of mechanical properties of dry, saturated and frozen porous rocks*. In: Shakoor A., Cato K. (eds) IAEG/AEG Annual Meeting Procs, San Francisco, California, 2018—Volume 6. Springer, Cham. Doi: 10.1007/978-3-319-93142-5_16
24. Hadi Keivani H., Samad Narimani Q., Vásárhelyi B. **Davarpanah M.** (2018): *Experimental study on hydraulic fracturing of homogenous and non-homogenous rock samples*. In: Török Á,; Görög P.; Vásárhelyi B. (eds), Mérnökgeológia-Kőzetmechanika 201-209.

6. REFRENCES[1]

ASTM 2005. Standard method of test for elastic moduli of rock core specimens in uniaxial compression. American Society for Testing and Materials

Bar, N., Weekes, G. (2017). Directional shear strength models in 2D and 3D limit equilibrium analyses to assess the stability of anisotropic rock slopes in the Pilbara region of Western Australia. Australian Geomechanics Journal. 52(4): 91-104.

Belikov, B.P., Alexandrov, K.S., Rysova, T.W. (1970). Upruie svoistva porodoobrasujscich mineralov I gornich porod. Izdat, Nauka, Moskva

Brace, W.F. (1964). Brittle fracture of rocks. State of Stress in the Earth's Crust (Ed. W.R. Judd), Elsevier, New York, 111-174.

Brace, W.F., Paulding, B.W., Scholz, C. (1966). Dilatancy in the fracture of crystalline rocks. Geophys. 71: 3939–3953.

Brontons, V., Tomás, R., Ivorra, S., Grediage, A., Martinez-Martinez, J., Benavente, D., Gomez-Heras, M. (2016). Improved correlation between the static and dynamic elastic modulus of different types of rocks. Materials & Structures 49(8): 3021-3037. https://doi.org/10.1617/s11527-015-0702-7

Brotons, V., Tomás, R., Ivorra, S., Grediaga, A. (2014). Relationship between static and dynamic elastic modulus of a calcarenite heated at different temperatures. Bull Eng Geol Environ 73:791–799.https://doi.org 10.1007/s10064-014-0583-y

Cai, M. (2010). Practical Estimates of Tensile Strength and Hoek–Brown Strength Parameter mi of Brittle Rocks". Rock Mech. Rock Eng. 43: 167-184. 2010. DOI: 10.1007/s00603-009-0053-1

Christaras, B., Auger, F., Mosse, E. (1994). Determination of the moduli of elasticity of rocks. Comparison of the ultrasonic velocity and mechanical resonance frequency methods with direct static methods. Mater Struct 27:222–228

[1] Thesis publications cited in list of publications.

Diederichs, M.S. (2003).The 2003 Canadian Geotechnical Colloquium: mechanistic interpretation and practical application of damage and spalling prediction criteria for deep tunnelling. Can. Geotech. J. 44: 1082–1116.

Dincer, I., Acar, A., Cobanoglu, A., Uras, U. (2004). Correlation between Schmidt hardness, uniaxial compressive strength and Young's modulus for andesites, basalts and tuffs. Bull Eng Geol Env 63:141–148. Doi: 10.1007/s10064-004-0230-0

Eissa, E.A., Kazi, A. (1988). Relation between static and dynamic Young's Moduli of rocks. Int J Rock Mech Min Sci. 25:479–482. https://doi.org/10.1016/0148-9062(88)90987-4

Gercek, H. (2007). Poisson's ratio values for rocks. Int. J. Rock Mech. Mining Sci. 44(1): 1–13. DOI: 10.1016/j.ijrmms.2006.04.011

Görög, P. (2007). Characterization and mechanical properties of the Eocene Buda Marl. Central European Geology. 50(3), 241–258.

Glamheden, R., Lindblom, U. (2002). Thermal and mechanical behaviour of refrigerated caverns in hard rock. Tunnelling and Underground Space Technology. Vol 17. pp 341-353.

Hawkins, A.B., McConnell, B.J. (1992). Sensitivity of sandstone strength and deformability to changes in moisture content". Q J Eng Geol 25(2): 115–130.

Haldane, JBS. (1919). The combination of linkage values and the calculation of distances between the loci of linked factors. Genetics 8:299–309.

Hoek, E., Brown, ET. (1997). Practical estimates of rock mass strength. Int J Rock Mech Min Sci 34(8):1165–1186. https://doi.org/10.1016/S1365-1609(97)80069-X

Hoek, E., Carter, TG., Diederichs, MS. (2013). Quantification of the geological strength index chart. 47th U.S. rock mechanics/geomechanics symposium, San Francisco, June 2013.

Hoek, E., Marinos, P. (2000). Predicting tunnel squeezing problems in weak heterogeneous rock masses. Tunnels and Tunnelling International 32(11):45-51

ISRM 2007. The Complete ISRM Suggested Methods for Rock Characterization, Testing and Monitoring:1974-2007, Edited by R. Ulusay & J.A. Hudson.

King, M.S. (1983). Static and dynamic elastic properties of rocks from Canadian Shield. Int. J. Rock Mech. Min. Sci 20(5): 237-241. https://doi.org/10.1016/0148-9062(83)90004-9

Kodama, J., Nishiyama, E., Kaneko,K.(2019). Measurement and interpretation of long-term deformation of rock slope at the Ikura limestone quarry, Japan. IntJ RockMechMinSci, 46:148–58.

Li, Z., Liu, S., Ren, W., Fang, J., Zhu, Q., Dun, Z. (2020). Multiscale Laboratory Study and Numerical Analysis of Water-Weakening Effect on Shale. Hindawi, Advances in Materials Science and Engineering. https://doi.org/10.1155/2020/5263431

Liu, B., Sun, Y., Wang, J., Zhang, G. (2020) Characteristic Analysis of Crack Initiation and Crack Damage Stress of Sandstone and Mudstone under Low-Temperature Condition. Journal of Cold Regions Engineering. https://doi.org/10.1061/(ASCE)CR.1943-5495.0000225

Lama, R.D., Vutukuri, V.S. (1978). Handbook on mechanical properties of rocks - Testing technique and results, Germany

Lógó, B.A.,Vásárhelyi, B. (2019). Estimation of the Poisson's Rate of the Intact Rock in the Function of the Rigidity. Periodica Polytechnica Civil Engineering 63: 1030-1037.

Mellor, M. (1971). Strength and deformability of rocks at low temperatures. USA Cold Regions Research and Engineering Laboratory, Research Report 294.

Mellor, M. (1973). Mechanical properties of rocks at low temperatures. In Permafrost: The North American Contribution to the 2nd International Conference on Permafrost, Yakutsk, 13-28 July, Washington D.C.: Natural Academy of Sciences.

McCann, D.M., Entwisle, D.C. (1992). Determination of Young's modulus of the rock mass from geophysical well logs. Geological Society Special Publication 65:317-325

Nicoll, S., Bar, N., Du, Plessis. (2017). Managing Risks on an Active Haul Road Adjacent to a Propagating Subsidence Zone at Telfer Gold Mine. Procedia Engineering. 191: 172-178.

Palchik, V. (2019). Simple stress–strain model of very strong limestones and dolomites for engineering practice. Geomech. Geophys. Geo-energ. Geo-resour. 6: 1-12.

Török, Á., Ficsor, A., Davarpanah, M., Vásárhelyi, B. (2018). Comparison of mechanical properties of dry, saturated and frozen porous rocks. IAEG/AEG Annual Meeting Proceedings, San Francisco, California, 6: 113-118.

Vásárhelyi, B., Davarpanah, M. (2018). Influence of Water Content on the Mechanical Parameters of the Intact Rock and Rock Mass. Periodica Polytechnica Civil Engng.62: 1060-1066.

Vásárhelyi, B., Ván, P. (2006). Influence of the water content for the strength of the rock. Eng. Geol. 84: 70-74.

Vásárhelyi, B. (2005). Statistical analysis of the influence of water content on the strength of the Miocene Limestone. Rock Mech. Rock Eng. 38: 69-76.

Vásárhelyi, B., Kovács, L., Török, Á. (2016). Analyzing the modified Hoek-Brown failure criteria using Hungarian granitic rock". Geomech. Geophys. Geo-energ. Geo-resour. 2:131–136. 2016.

Yang, H., Shan, R., Zhang, j., Wub, F., Guo, Z. (2018). Mechanical properties of frozen rock mass with two diagonal intersected fractures. Int. J. Mining Sci. Techn. 28: 631-638

Yagiz, S.(2011). P-wave velocity test for the assessment of some geotechnical properties of rock materials. Bull Mater Sci (34), 943–957

Zhao, Y.S., Wan, Z.J., Feng, Z.J. (2017). Evolution of mechanical properties of granite at high temperature and high pressure Geomech. Geophys. Geo-energ. Geo-resour. 3:199. https://doi.org/10.1007/s40948-017-0052-8